RSC Advances

PAPER

View Article Online
View Journal | View Issue

Cite this: *RSC Adv.*, 2023, **13**, 7818

Nickel–palladium bimetallic nanoparticles supported on multi-walled carbon nanotubes; versatile catalyst for Sonogashira cross-coupling reactions†

Katherine A. Wilson, Lacey A. Picinich and Ali R. Siamaki *

We have developed an efficient method to generate highly active nickel–palladium bimetallic nanoparticles supported on multi-walled carbon nanotubes (Ni–Pd/MWCNTs) by dry mixing of the nickel and palladium salts utilizing the mechanical energy of a ball-mill. These nanoparticles were successfully employed in Sonogashira cross-coupling reactions with a wide array of functionalized aryl halides and terminal alkynes under ligand and copper free conditions using a Monowave 50 heating reactor. Notably, the concentration of palladium can be lowered to a minimum amount of 0.81% and replaced by more abundant and less expensive nickel nanoparticles while effectively catalyzing the reaction. The remarkable reactivity of the Ni–Pd/MWCNTs catalyst toward Sonogashira cross-coupling reactions is attributed to the high degree of the dispersion of Ni–Pd nanoparticles with small particle size of 5–10 nm due to an efficient grinding method. The catalyst was easily removed from the reaction mixture by centrifugation and reused several times with minimal loss of catalytic activity. Furthermore, the concentration of catalyst in Sonogashira reactions can be reduced to a minimum amount of 0.01 mol% while still providing a high conversion of the Sonogashira product with a remarkable turnover number (TON) of 7200 and turnover frequency (TOF) of 21 600 h^{-1}. The catalyst was fully characterized by a variety of spectroscopic techniques including X-ray diffraction (XRD), transmission electron microscopy (TEM) and X-ray photoelectron spectroscopy (XPS).

Received 3rd January 2023
Accepted 26th February 2023

DOI: 10.1039/d3ra00027c

rsc.li/rsc-advances

Introduction

Sonogashira cross-coupling reaction is a powerful method for the formation of a carbon–carbon bond between an aryl halide and terminal alkyne and has found a broad range of applications in the synthesis of natural products,[1–3] heterocyclic compounds,[4–6] optical and electronic molecular structures,[7–9] biological active pharmaceuticals,[10] and many others.[11–14] These reactions typically involve the use of a palladium catalyst along with a copper cocatalyst under homogeneous conditions utilizing a ligand to stabilize the metal and enhance the catalytic activity.[15–17] However, the issues associated with homogeneous catalysis such as difficulty in separation of the catalyst from the reaction mixture which result in residual metal contamination in the final product as well as a lack of recyclability remain a major challenge for large-scale application of this reaction in terms of pharmaceutical and industrial scope.[18,19] In addition, the use of copper as the cocatalyst initiates the oxidative homocoupling of the terminal alkyne (Glaser coupling) to produce the corresponding diyne byproduct,[20–22] a significant drawback which prompted attention to developing copper free Sonogashira coupling.[23,24] Heterogeneous catalysis is an alternative attractive approach to construct carbon–carbon bonds in which the metal is fixed on solid supports such as zeolites,[25–27] polymers,[28–30] mesoporous silica,[31,32] and carbon materials.[33] This provides a unique platform to influence the stability and reactivity of these materials along with ease of separation, simple recovery, and recyclability demonstrated by significant research efforts in this area in recent years.[33–35]

Carbon nanotubes (CNTs) have recently been considered as potential support systems for metal-catalyzed carbon–carbon applications.[36,37] Due to high surface area (2600 m^2 g^{-1}), extended π system, and thermal stability, CNTs exhibit excellent tunability in supporting a variety of metallic and bi-metallic systems in heterogeneous catalysis.[38,39] In addition, other properties of CNTs such as high thermal, chemical, and mechanical stability as well as hollow structure also represent desirable characteristics as 2D support layers in catalytic reactions. In this regard, multi-walled carbon nanotubes (MWCNTs) consist of multiple graphene layers with a diameter ranging from 2 to 25 nm and 0.34 nm distance between each sheet with

Department of Chemistry, Physics, and Materials Science, Fayetteville State University, Fayetteville, NC, USA 28301. E-mail: asiamaki@uncfsu.edu

† Electronic supplementary information (ESI) available: General methods, additional characterization data, ^1H and ^{13}C NMR Spectra, and other supporting materials are available. See DOI: https://doi.org/10.1039/d3ra00027c

extended surface area exhibit superior activity as the catalyst support in cross coupling reactions compared to other type of CNTs materials.[40–44]

We recently reported the extraordinary cross-coupling catalytic activity of MWCNTs supported palladium nanoparticles (Pd/MWCNTs)[45] and magnetic nickel–Fe_3O_4 (Ni–Fe_3O_4/MWCNTs)[46] which were prepared using straightforward solventless mechanochemical mixing using a ball-mill. These supported nanoparticles demonstrated excellent reactivity and reusability for Suzuki cross coupling reactions. The dry mixing preparation provides sufficient mechanical energy for aggressive ball-milling of the precursor metal salts and carbon nanotubes blending to facilitate partial decomposition of the materials into ultra fine nanoparticles (5–10 nm) without the need for additional heating or using any chemical reducing agent.[47,48] Encouraged by these results, we were determined to further investigate the potential utility of this method to prepare other useful bimetallic nanoparticles supported on MWCNTs for cross coupling catalysis such as Sonogashira coupling reactions.

Bimetallic nanoparticles have been of considerable interest in recent years due to enhanced catalytic activity, selectivity, and stability for various cross coupling reactions.[49–55] Introducing the second metal, usually a more abundant and less expensive element reduces the cost associated with the use of precious metal due to using a lower amount of palladium in preparation, while still providing a catalyst with similar electronic structure and improved reactivity.[56–58] In this regard, nickel is considered as one of the potential alternatives to palladium due to its similar electronic structure and the ability to undergo oxidative addition, high bonding affinity, and flexibility in forming multiple oxidation states.[59–61] In addition, nickel is as reactive as palladium in metal catalyzed cross coupling reactions. Therefore, nickel will be an ideal and affordable alternative source for the preparation of catalyst necessary for cross coupling reactions.[62–66] Nickel salts such as $Ni(NO_3)_2$, $Ni(OAc)_2$, and $Ni(acac)_2$ are less expensive and readily available, compare to the most palladium salts. The cost of nickel in its elemental form is much lower than palladium. Although a variety of nickel complexes has been developed as efficient new homogeneous systems for carbon–carbon bonds, the use of these catalysts under homogeneous conditions has limited their commercial viability due to product contamination as a direct result of inability to effectively separate the catalyst from the reaction product.[67–72]

Herein, we report the preparation of nickel–palladium bimetallic nanoparticles supported on MWCNTs (Ni–Pd/MWCNTs) *via* simple mixing of the corresponding nickel and palladium salts under a mechanical energy of the ball-mill mixing and its application in Sonogashira coupling reaction of variously functionalized aryl halides and terminal alkyne using Monowave 50 heating reactor. Notably, the amount of the palladium in this solventless preparation can be lowered as minimum as 0.81 wt% while still achieving a high conversion (95%) and recyclability in Sonogashira reactions. In addition, The Monowave 50 reactor provides an effective heating source by which the reactions can be completed in a safe and sealed glass vessel under monitored temperature and pressure with continuous magnetic stirring affording the high yields of the products at 120 °C in a short reaction time. The low palladium loading and recyclability of the catalyst makes this an affordable and clean option for pharmaceutical and industrial applications. The method presented here is facile, cost efficient and environmentally friendly, allowing for large scale preparation of Ni–Pd/MWCNTs nanoparticles to achieve often challenging Sonogashira coupling reactions.

Results and discussion

Concentration of nickel/palladium on catalysis

To examine the effect of nickel and palladium nanoparticles loading ratios on MWCNTs support toward the catalysis in Sonogashira coupling reactions, four different catalytic systems

Table 1 Preparation of the catalyst for Sonogashira cross-coupling reaction[a]

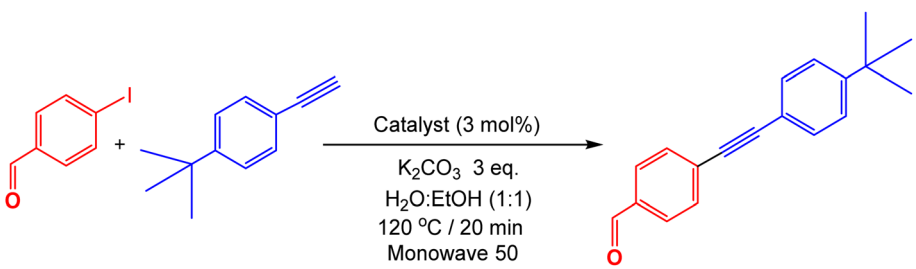

Catalyst #	Catalyst	Ni (wt%)	Pd (wt%)	MWCNTs (wt%)	Conversion[b] %
Catalyst 1	Ni/MWCNTs	10(8.2)[c]	0	90	15
Catalyst 2	Ni–Pd/MWCNTs	10(8.5)[c]	10(7.8)[c]	80	100
Catalyst 3	Ni–Pd/MWCNTs	10(7.9)[c]	1(0.81)[c]	89	95
Catalyst 4	Pd/MWCNTs	0	1(0.86)[c]	99	70

[a] 4-Iodobenzaldehyde (50 mg, 0.22 mmol, 1 eq.), 4-*tert*-butylphenylacetylene (41.7 mg, 0.26 mmol, 1.2 eq.), potassium carbonate (91.1 mg, 0.66 mmol, 3 eq.), and nanoparticles catalysts (6.6 μmol, 3 mol%) in a mixture of 4 mL of H_2O : EtOH (1 : 1) were heated at 120 °C for 20 minutes using Monowave 50 heating reactor. [b] Conversion % were determined by GC-MS. [c] Concentrations in parentheses were determined by ICP-MS.

were prepared. Table 1 reveals the effect of concentration of palladium and nickel nanoparticles supported on MWCNTs on catalytic activity in Sonogashira coupling reaction of 4-iodobenzaldehyde and 4-*t*-butylphenyl acetylene using potassium carbonate as the base and a mixture of water : ethanol as solvent. The reaction was heated at 120 °C for 20 minutes in Monowave 50 heating reactor. The actual metal contents in all catalysts were determined by means of inductively coupled plasma equipped with mass spectroscopy (ICP-MS) and amounted to be for catalyst 1, 8.2% of nickel, catalyst 2, Ni: 8.5%, Pd: 7.8%, catalyst 3, Ni: 7.9%, Pd: 0.81%, and catalyst 4, Pd: 0.86%.

While the catalyst 1, Ni/MWCNTs having 8.2% nickel content by ICP-MS with no palladium added only afforded 15% conversion of Sonogashira product (entry 1), with both nickel and palladium content of 8.5% and 7.8% each respectively (catalyst 2), the reaction provided a quantitative conversion (entry 2). Interestingly, reducing the concentration of Pd to 0.81% while having 7.9% of nickel (catalyst 3), the reaction can be completed smoothly giving a relatively high conversion of the product (95%). Notably, the Pd/MWCNTs having 0.86% Pd content (catalyst 4) with no nickel only afforded 70% conversion to the product. The combination of Ni–Pd/MWCNTs in catalyst 3 provides an ideal platform to design a bimetallic nanoparticle

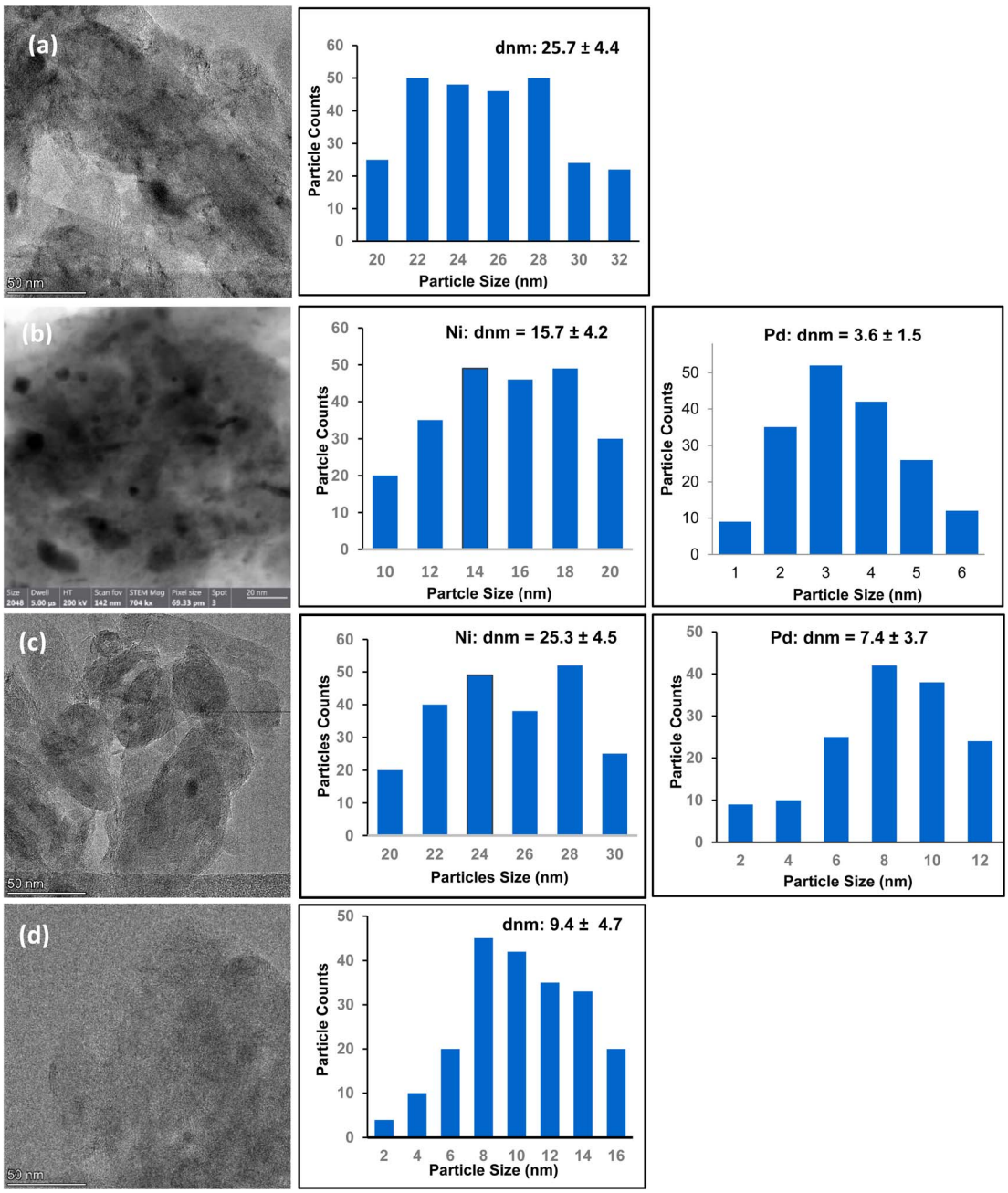

Fig. 1 TEM images and particle size distributions (a) catalyst 1 (Ni/MWCNTs), (b) catalyst 2 (Ni–Pd/MWCNTs, 7.8% Pd) (c) catalyst 3 (Ni–Pd/MWCNTs, 0.81% Pd), (d) catalyst 4 (Pd/MWCNTs, 0.86% Pd).

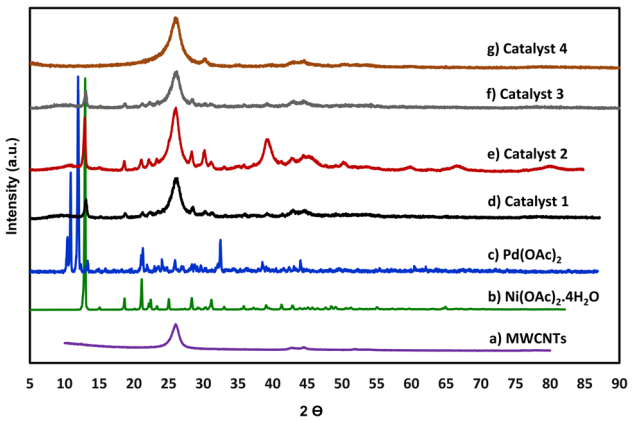

Fig. 2 XRD image of catalysts 1–4 (d–g), original salts (b and c), and MWCNTs (a).

supported on CNTs in which the amount of palladium as the noble metal is lowered to a minimum amount of 0.81% and replaced by more abundant and less expensive nickel nanoparticles while still providing high catalytic activity in Sonogashira coupling reaction.

The TEM images of all four catalysts in Table 1 are depicted in Fig. 1. Catalyst 1 (Ni/MWCNTs) shows significant aggregation of nickel nanoparticles on the surface of MWCNTs with the average size of particles around 25.7 ± 4.4 nm (Fig. 1a). For catalyst 2, both nickel and palladium nanoparticles are uniformly distributed on the surface of multi-walled carbon nanotubes (Fig. 1b). In this system, it is found from the TEM images that nickel nanoparticles are mostly located inside the tubes while the palladium particles are concentrated on the surface of the nanotubes. The average particle size for nickel nanoparticle were identified as 15.7 ± 4.2 nm whereas the average particle size for palladium particles is measured to be 3.6 ± 1.5 nm. The high dispersion of nickel and palladium nanoparticles on the surface of nanotubes imply the effect of mixing the metal salts during the mechanical shaking in the ball-mill to produce ultrafine mixture of Ni–Pd/MWCNTs materials. In catalyst 3, the elemental nickel particles were much larger, with an average particle size of 25.3 ± 4.5 nm in diameter and also relatively dispersed across the tubes. The palladium nanoparticles in this catalyst were also small, with an average particle size of 7.4 ± 3.7 nm with even dispersion across the nanotubes (Fig. 1c). There are also some evidence for the presence of nickel oxide intermixed with nickel particles with diameter around 15.3 nm in this sample. It is clear that both catalyst 2 and 3 show good dispersion of nanoparticles on multiwalled carbon nanotubes (MWCNTs) but catalyst 2 shows slightly lower particle size for Pd nanoparticles. Catalyst 4 which only contains 0.86% of Pd nanoparticles demonstrates an average particle size of 9.4 ± 4.7 nm with even distribution on the surface of solid support (Fig. 1d).

The as-prepared nanoparticles in Table 1 were also characterized by X-ray diffraction (XRD) to elucidate further insight into the structure of these nanoparticles. Fig. 2 displays the XRD pattern of catalysts 1–4 nanoparticles as well as the XRD patterns of the original samples of $Ni(OAc)_2 \cdot 4H_2O$, $Pd(OAc)_2$, and MWCNTs. For example, the peak at 2θ value of 40.1° corresponds to the (111) d-spacing of 2.2 Å of metallic Pd indicating the decomposition of metal salt under mechanochemical energy of ball mill. The broadening of the peaks was due to the nanoscale nature of the crystalline phase. The presence of peaks at 40.1°, 43.2°, 50.2°, and 60.1° could be attributed to the corresponding (111), (200), (220), (311), and (222) planes for nickel oxide nanoparticles. This will suggest that under the ball-mall energy some of the Ni salts have been converted to nickel oxide nanoparticles. The broad shoulder at 45° can be identified as small amount of Ni (111) phase. The small and broad peak at 26.3° is the characteristic diffraction of MWCNTs. Catalyst 2 show higher intensities of the Pd peaks relative to catalyst 3 in accordance with higher Pd content in this catalyst (7.8%). Catalyst 4 displays weak signal intensities for Pd due to low level of Pd composition in this sample (0.86%). Catalyst 1 also demonstrates the presence of peaks for nickel oxide nanoparticles formation on the surface of MWCNTs. Furthermore, in all catalyst samples, the XRD pattern of the original residual metal salts is slightly noticeable in the product indicating the partial decomposition of the original metal salts using the mechanical energy of the ball-mill at room temperature.

The surface chemical composition of catalysts was investigated by means of XPS analysis (Fig. 3). The survey spectra demonstrate the presence of nickel, palladium, oxygen, and carbon in these nanoparticles (ESI†). The Ni 2p spectra of the

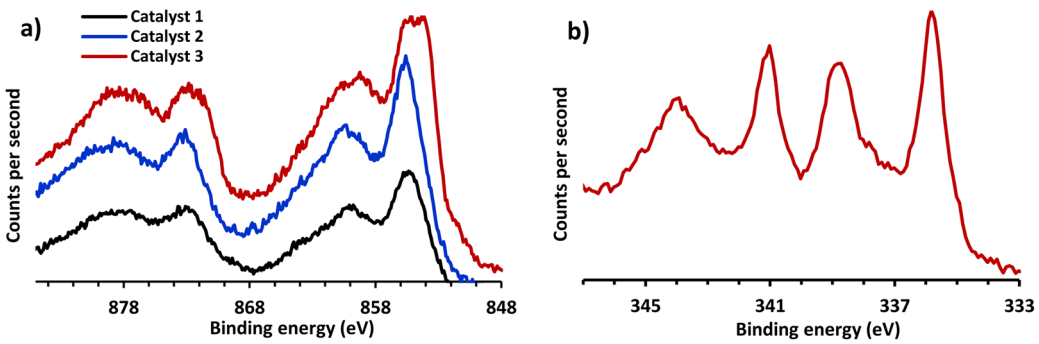

Fig. 3 XPS data of Ni–Pd/MWCNTs nanoparticles (a) Ni binding energy catalysts 1–3 (b) Pd binding energy catalyst 2.

Table 2 Recyclability of catalysts 2 and 3 in Sonogashira cross-coupling reaction[a]

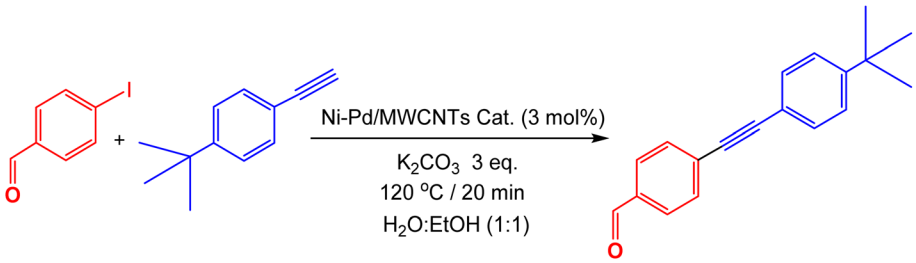

Run	Conversion[b] % catalyst 2	Conversion[b] % catalyst 3
1	100	95
2	100	82
3	96	75
4	91	54
5	90	—
6	85	—

[a] 4-Iodobenzaldehyde (50 mg, 0.22 mmol, 1 eq.), 4-*tert*-butylphenylacetylene (41.7 mg, 0.26 mmol, 1.2 eq.), potassium carbonate (91.1 mg, 0.66 mmol, 3 eq.) and Ni–Pd/MWCNTs nanoparticles (catalyst 2 and 3) (6.6 μmol, 3 mol%) in a mixture of 4 mL H_2O : EtOH (1 : 1) were heated at 120 °C for 20 minutes using Monowave 50 heating reactor. [b] Conversion % were determined by GC-MS.

surface composites are shown in Fig. 3a for catalyst 1–3. The Ni spectra around 855 eV ($2p_{3/2}$) and 873 eV ($2p_{1/2}$) indicate the presence of Ni(II) perhaps in the form of nickel oxide. The broadness of the peak at lower binding energy around 853 eV can be attributed to the formation of small amount of metallic Ni $2p_{3/2}$ due to a partial reduction of the nickel salt during the ball mill process. This is more evident for catalyst 2 (Fig. 3a). The XPS spectrum of Ni–Pd/MWCNTs exhibit the presence of two important Pd species in catalyst 2 (Fig. 3b). The binding energy of the Pd $3d_{5/2}$ measured at 335.8 eV and $Pd_{3/2}$ 341 eV indicate the presence of Pd(0), while the binding energy of $Pd_{5/2}$ at 338.6 eV and $Pd_{3/2}$ at 343.9 eV related to Pd(II) oxidation state. It is evident from these data that the corresponding peaks for both metals in this bimetallic catalyst 2 slightly shifted toward the higher binding energies compared to monometallic catalyst. Addition of nickel to palladium has demonstrated a significant improvement in catalytic activities.[73,74] This may suggest an interaction between Pd and Ni possibly in the form of electron transfer from Ni to Pd consistent with the reported data.[75–77] Such interaction may change the electronic structure of Pd and lead to the formation of more Pd(0) on the surface of MWCNTs, a feature which could influence the catalytic activity of Ni–Pd/MWCNTs nanoparticles in Sonogashira coupling reaction albeit having a small amount of Pd content. Noteworthy, due to the low concentration of Pd in catalyst 3 (0.81%), we were unable to obtain a clear XPS data for Pd nanoparticles in this catalyst.

Catalyst recycling

Due to the greater catalytic activities (Table 1), catalyst 2 and 3 were used to examine the recyclability of these nanoparticles under Sonogashira coupling reactions. As shown in Table 2, the reaction of 4-iodobenzaldehyde with 4-*tert*-butylphenyl acetylene in a mixture of water : ethanol as the solvent and in the presence of potassium carbonate as the base with 3 mol% of the catalyst afforded a quantitative conversion of Sonogashira product after heating at 120 °C for 20 min using Monowave 50 heating reactor. The catalyst was effectively removed from the reaction mixture by centrifugation and reused for subsequent run. In this case, quantitative conversions were obtained in the first two runs. The catalytic activity was slightly dropped in run 3 yielding 96% conversion and further dropped in runs 4 and 5 to about 90% and run 6 to give 85% conversion. Catalyst 3 demonstrated a lower conversion % in run 2 and 3 with 82% and 75%, respectively. The decrease in recyclability of this catalyst can be attributed to lower concentration of Pd (0.86%) in these nanoparticles.

Table 3 Effect of catalyst loading on catalysis using catalysts 2 and 3[a]

Catalyst loading (mol%)	Conversion[b] % catalyst 2	Conversion % catalyst 3
3	100	95
1.5	100	90
0.8	100	72
0.4	100	58
0.2	98	—
0.1	92	—
0.05	80	—
0.01	72	—

[a] 4-Iodobenzaldehyde (50 mg, 0.22 mmol, 1 eq.), 4-*tert*-butylphenylacetylene (41.7 mg, 0.26 mmol, 1.2 eq.), potassium carbonate (91.1 mg, 0.66 mmol, 3 eq.) and Ni–Pd/MWCNTs nanoparticles (catalyst 2 and 3) (as indicated) in a mixture of 4 mL of H_2O : EtOH (1 : 1) were heated at 120 °C for 20 minutes using Monowave 50 heating reactor. [b] Conversion % were determined by GC-MS.

Table 4 Diversity of the Sonogashira cross-coupling reactions using catalyst 3[a]

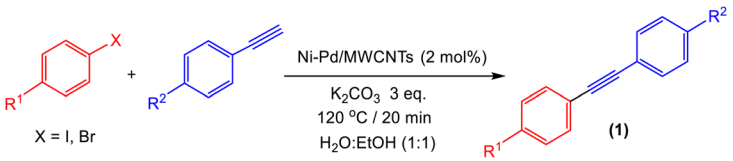

cpd	Aryl-halide	Alkyne	1(%)[b]
a	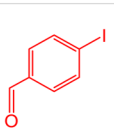	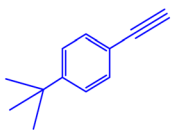	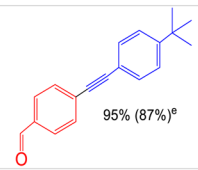 95% (87%)[e]
b	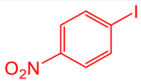	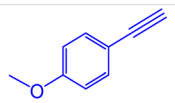	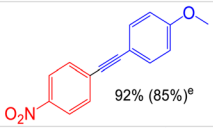 92% (85%)[e]
c		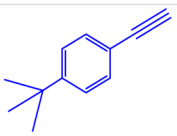	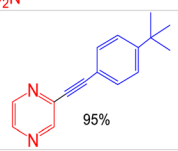 95%
d	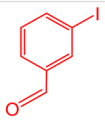	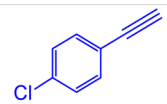	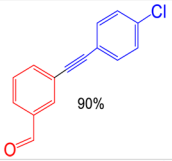 90%
e	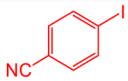	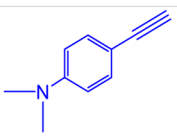	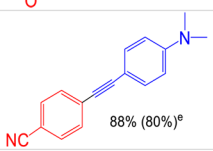 88% (80%)[e]
f[c]	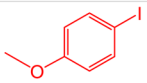	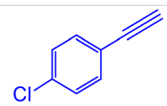	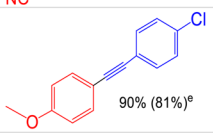 90% (81%)[e]
g	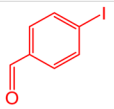	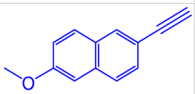	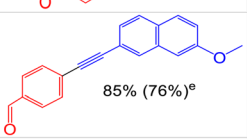 85% (76%)[e]
h	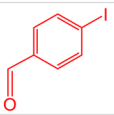	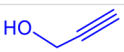	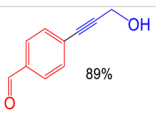 89%
i	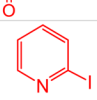	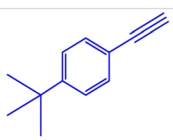	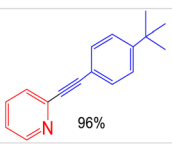 96%
j[d]	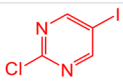	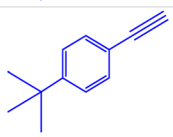	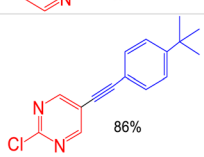 86%

[a] Aryl halides (0.25 mmol, 1 eq.), terminal alkyne (0.3 mmol, 1.2 eq.), potassium carbonate (0.75 mmol, 3 eq.) and Ni–Pd/MWCNTs nanoparticles (catalyst 3) (7.50 mg, 5.0 μmol, 2 mol%) in a mixture of 4 mL H_2O : EtOH (1 : 1) were heated at 120 °C for 15 minutes using Monowave 50 heating reactor. [b] Isolated yield. [c] Reaction was heated at 150 °C for 30 min in Monowave 50 sealed tube. [d] *tert*-Butanol (4 mL) was used as the only solvent. [e] Yields in this parathesis correspond to the use of aryl bromide.

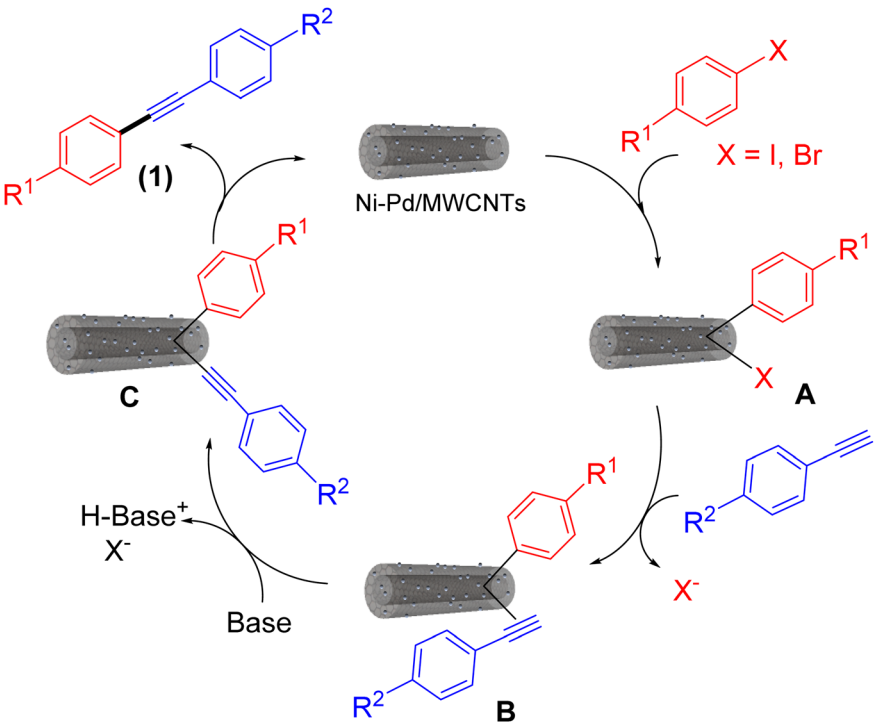

Fig. 4 Mechanism of Sonogashira cross-coupling reaction.

Effect of catalyst loading

The catalytic activities of catalyst 2 and 3 toward Sonogashira cross-coupling reaction of 4-iodobenzaldehyde and 4-*t*-butylphenyl acetylene using potassium carbonate as the base heated at 120 °C for 20 minutes in Monowave 50 reactor using water : ethanol as solvent were investigated by using various concentrations of this catalyst (Table 3). These results indicate that the catalyst 2 can successfully catalyze the reaction at lower concentration of 0.1 mol% affording 92% product. Further decrease in the concentration of the catalyst to 0.05 mol% and 0.01 mol% provided lower conversion % of 80% and 72%, respectively. The latter indicates an excellent catalytic activity of these bimetallic nanoparticles at a very low catalyst loading in Sonogashira reactions achieving a turnover number (TON) of 7200 and turnover frequency (TOF) of 21 600 h^{-1}. With catalyst 3, we were able to obtain a minimum of 58% conversion % using 0.4 mol% of the catalyst concentration.

Diversity of substrates in Sonogashira reactions

Catalyst 3 nanoparticles were successfully employed to prepare other Sonogashira coupling products having a diverse range of functional groups on both aryl halides and terminal alkynes in excellent yields. As illustrated in Table 4, these reactions were completed using 2 mol% of the catalyst at 120 °C for 20 minutes using Monowave 50 heating reactor with water : ethanol as the solvent. Aryl iodide bearing the electron withdrawing functional groups such as aldehyde (**1a**), nitro group (**1b**), nitrile (**1e**) produces the corresponding products in high yield. In contrast, the electron donor methoxy group (**1f**) can also be easily introduced into the structures. Interestingly, the heterocyclic structures including pyrazine (**1c**), pyridine (**1i**) and pyrimidine (**1j**) can be effectively applied into the coupling products. These important nitrogen containing molecules which are the basis of many biological and pharmaceutical active products can be prepared in high yield using the as prepared Ni–Pd/MWCNTs nanoparticles. Similarly, a broad range of diversity can be altered from the terminal alkyne end using alkyl (**1a**), methoxy (**1b**), dimethylamino (**1e**), and propargyl alcohol (**1h**). Notably, the bromo-substituted arenes (**1a**, **1b**, **1e**, **1f**, **1g**) can also be added in these coupling reactions providing a good, isolated yield of the Sonogashira products.

A plausible mechanism can be envisioned for the Sonogashira cross-coupling reaction utilizing Ni–Pd/MWCNTs nanoparticles based on the reported studies.[16] As shown in Fig. 4, oxidative addition of aryl halide to Ni–Pd bimetallic nanoparticles generates the intermediate **A**. Alkyne π-coordination followed by deprotonation in the presence of base forms intermediates **B** and **C**, respectively. Reductive elimination of **C** produces the final coupling product (**1**) and regenerate the catalyst for the next catalytic cycle.

Conclusions

In summary, we have prepared a bimetallic system consist of nickel and palladium nanoparticles supported on muti-walled carbon nanotubes (Ni–Pd/MWCNTs) by dry mixing of the nickel and palladium salts under mechanical shaking of a ball-mill. The method is straightforward and simple and allows for instant preparation of the material in large amount. Notably, the concentration of palladium in bimetallic combination of Ni–Pd can be reduced as low as 0.81% (ICP-MS analysis) and replaced

with more abundant and less expensive nickel nanoparticles while still maintaining a great catalytic performance. The catalyst 3 (7.9% Ni, 0.81% Pd) nanoparticles exhibited excellent catalytic activity Sonogashira cross-coupling reactions utilizing diverse range of functional groups on both aryl halides and terminal alkynes without the necessity of ligand and copper co-catalyst. The catalyst can be recycled effectively multiple times with minimum loss of reactivity. Furthermore, the concentration of catalyst in Sonogashira reactions can be reduced to a minimum amount of 0.01 mol% while still providing a high conversion of the Sonogashira product with a remarkable turnover number (TON) of 7200 and turnover frequency (TOF) of 21 600 h^{-1}. The catalytic system prepared by this simple and solventless approach provides a facile, cost-efficient, and direct method for large scale preparation of an effective Ni–Pd/MWCNTs nanoparticles to accomplish often-challenging ligand and copper free Sonogashira cross coupling reactions, a feature that is of considerable importance for pharmaceutical and industrial applications.

Experimental

Nickel(II) acetate tetrahydrate and palladium acetate were obtained from Sigma-Aldrich. Aryl iodides and bromides, and functionalized terminal alkynes were purchased from MilliporeSigma, Alfa Aesar, and ACROS Organics and used as received. Multi-walled carbon nanotubes (MWCNTs) 50–85 nm was purchased from Graphene Supermarket. A mixture of ethanol–deionized water was used as the solvent system for all the reactions. Transmission electron microscopy was performed on ThermoFisher Talos F200X G2, a 200 kV FEG (Field Emission Gun) Analytical Scanning Transmission Electron Microscope (S/TEM). X-ray diffraction (XRD) was accomplished on Rigaku MiniFlex 600 X-ray diffractometer. X-ray photoelectron spectroscopy (XPS) was performed on Kratos Axis Supra X-ray photoelectron spectrometer. Inductively Coupled Plasma-Mass Spectrometry (ICP-MS) analysis was completed using NexION 300D (PerkinElmer, Inc.). Gas Chromatography-Mass Spectroscopy (GC-MS) of organic products was analyzed using a Shimadzu GC-MS QP2010 SE. ^{1}H and ^{13}C NMR spectra were acquired on a JEOL 400 MHz spectrometer equipped with autosampler. All Sonogashira cross-coupling reactions were performed using Anton-Paar Monowave 50 heating reactor.

Preparation of Ni–Pd/MWCNTs nanoparticles

To examine the effect of Ni and Pd nanoparticles ratios and the loading of nanoparticles on MWCNTs support on the catalysis in Sonogashira coupling reactions, four different catalytic systems were prepared as follows:

Catalyst 1. Nickel acetate tetrahydrate (42.39 mg, 10% Ni content) and multi-walled carbon nanotubes (MWCNTs) (90 mg) were mixed in a 20 mL volume zirconium ceramic vial (SPEX CertiPrep). After adding two zirconium balls, the vial was subjected to mechanical shaking using SPEX 8000M ball-mill mixer for 45 min mixer with 1060 cycles per minutes with 5.9 cm back and forth and 2.5 cm side to side mechanical movements. The final product of (Ni/MWCNTs) nanoparticles were obtained as black powder. Similar ball-mill procedures were used for the preparation of other Ni–Pd/MWCNTs using different concentration of nickel and palladium as follows:

Catalyst 2. Ni–Pd/MWCNTs (10% Ni, 10% Pd): nickel acetate tetrahydrate (42.39 mg, 10% Ni content), palladium acetate (21.13 mg, 10% Pd content), and multi-walled carbon nanotubes (MWCNTs) (80 mg).

Catalyst 3. Ni–Pd/MWCNTs (10% Ni, 1% Pd): nickel acetate tetrahydrate (42.39 mg, 10% Ni content), palladium acetate (2.11 mg, 1% Pd content), and multi-walled carbon nanotubes (MWCNTs) (89 mg).

Catalyst 4. Pd/MWCNTs (1% Pd): palladium acetate (2.11 mg, 1% Pd content), and multi-walled carbon nanotubes (MWCNTs) (99 mg).

The actual metal contents in all catalysts (1–4) were determined by means of inductively coupled plasma equipped with mass spectroscopy (ICP-MS). For this purpose, a solution of 70% HNO_3 (0.5 mL) was added to 20 mg of each catalyst sample and kept at 70 °C overnight. Concentrated HCl (1.5 mL) was added to this mixture and incubated further at 70 °C overnight. The entire catalyst sample was diluted with 2% nitric acid and subjected to ICP-MS analysis. The metal contents were determined to be for catalyst 1, 8.2% of nickel, catalyst 2, Ni: 8.5%, Pd: 7.8%, catalyst 3, Ni: 7.9%, Pd: 0.81%, and catalyst 4, Pd: 0.86%.

Procedure for recycling the Ni–Pd/MWCNTs

4-Iodobenzaldehyde (50 mg, 0.22 mmol, 1 eq.) and 4-*tert*-butylphenylacetylene (41.7 mg, 0.26 mmol, 1.2 eq.) were added to a mixture of water : ethanol (4 mL) in 10 mL Monowave 50 vial. To this was added potassium carbonate (91.1 mg, 0.66 mmol, 3 eq.) and Ni–Pd/MWCNTs nanoparticles catalyst 2 or catalyst 3 (6.60 μmol, 3 mol%). The reaction was sealed and heated at 120 °C for 20 minutes in Monowave 50 heating reactor. After the reaction was completed, the reaction solution was diluted with ethanol (4 mL), dichloromethane (4 mL), and the entire mixture was centrifuged for 5 minutes at 5000 RPM. The aqueous solution was decanted and the organic layer including dichloromethane was combined to give the Ni–Pd/MWCNTs nanoparticles as a precipitate. This procedure was repeated twice to ensure the removal of all organic materials from the surface of the catalyst. The clean catalyst was reused for the subsequent reaction by adding fresh reagents. The recycling procedure was repeated for every run and the formation of product was analyzed by GC-MS spectroscopy.

Procedure for Sonogashira cross-coupling reactions

Substituted aryl halides (0.25 mmol, 1 eq.) and terminal alkynes (0.3 mmol, 1.2 eq.) were added to a mixture of water : ethanol (4 mL) and placed in 10 mL Monowave 50 vial. After adding potassium carbonate (0.75 mmol, 3 eq.) and catalyst 3 (7.50 mg, 5.0 μmol, 2 mol%), the reaction mixture was heated at 120 °C for 20 minutes (or the time indicated in Table 4) in Monowave 50 heating reactor in a sealed vial. Upon the completion of the reaction, the mixture was extracted with dichloromethane (2 × 5 mL). The organic layers were combined, dried over sodium

sulfate, and filtered. The solvent was removed *in vacuo* and the final products was purified by flash chromatography on silica gel using hexane: ethyl acetate as the eluent.

Author contributions

A. R. S. supervised the project, analyzed the data, and wrote the paper. K. A. W. and L. A. P. equally contributed to the experimental work, analysis, and reaction development. All authors have read and agreed to the published version of the manuscript.

Conflicts of interest

The authors declare no conflict of interest.

Acknowledgements

We thank the NSF-HBCU-UP RIA grant 2101126 for funding this project. The authors gratefully acknowledge the Analytical Instrumentation Facilities at University of North Carolina at Chapel Hill (CHANL) and North Carolina State University (AIF) for the XPS and TEM analysis. We are also indebted to Dr Carrie Donley at CHANL for her assistance and discussion about XPS data. The authors also thank SENCR-MIC at Fayetteville State University for the use of X-ray Diffraction (XRD).

References

1 D. Wang and S. Gao, *Org. Chem. Front.*, 2014, **1**, 556–566.
2 R. Chinchilla and C. Nájera, *Chem. Rev.*, 2007, **107**, 874–922.
3 R. Chinchilla and C. Nájera, *Chem. Soc. Rev.*, 2011, **40**, 5084–5121.
4 M. M. Heravi and S. Sadjadi, *Tetrahedron*, 2009, **65**, 7761–7775.
5 M. M. Heravi, M. Ghanbarian, N. Ghalavand and N. Nazari, *Curr. Org. Chem.*, 2018, **22**, 1420–1457, DOI: **10.2174/1385272822666180322122232**.
6 G. Albano and L. A. Aronica, *Catalysts*, 2020, **10**, 25.
7 S. M. McAfee, J. R. Cann, P. Josse, P. Blanchard, C. Cabanetos and G. C. Welch, *ACS Sustainable Chem. Eng.*, 2016, **4**, 3504–3517.
8 L. Brunsveld, E. W. Meijer, R. B. Prince and J. S. Moore, *J. Am. Chem. Soc.*, 2001, **123**, 7978–7984.
9 M. Sonoda, A. Inaba, K. Itahashi and Y. Tobe, *Org. Lett.*, 2001, **3**, 2419–2421.
10 C. Torborg and M. Beller, *Adv. Synth. Catal.*, 2009, **351**, 3027–3043.
11 B. Li, Y. Fu, Y. Han and Z. Bo, *Macromol. Rapid Commun.*, 2006, **27**, 1355–1361.
12 T. Hagiwara, Y. Murano, Y. Watanabe, T. Hoshi and T. Sawaguchi, *Tetrahedron Lett.*, 2012, **53**, 2805–2808.
13 S. Hoger, S. Rosselli, A. D. Ramminger and V. Enkelmann, *Org. Lett.*, 2002, **4**, 4269–4272.
14 K. Onitsuka, M. Fujimoto, N. Ohshiro and S. Takahashi, *Angew. Chem., Int. Ed.*, 1999, **38**, 689–692.
15 A. M. Thomas, A. Sujatha and G. Anilkumar, *RSC Adv.*, 2014, **4**, 21688–21698.
16 M. Karak, L. C. A. Barbosa and G. C. Hargaden, *RSC Adv.*, 2014, **4**, 53442–53466.
17 M. Bakherad, *Appl. Organomet. Chem.*, 2013, **27**, 125–140.
18 R. J. Lundgren and M. Stradiotto, *Chem.–Eur. J.*, 2012, **18**, 9758–9769, DOI: **10.1002/chem.201201195**.
19 M. Pagliaro, V. Pandarus, R. Ciriminna, F. Béland and P. Demma Carà, *ChemCatChem*, 2012, **4**, 432–445, DOI: **10.1002/cctc.201100422.19**.
20 G. Evano, N. Blanchard and M. Toumi, *Chem. Rev.*, 2008, **108**, 3054–3131.
21 I. Kanwal, A. Mujahid, N. Rasool, K. Rizwan, A. Malik, G. Ahmad, S. A. Ali Shah, U. Rashid and N. M. Nasir, *Catalysts*, 2020, **10**, 443, DOI: **10.3390/catal10040443**.
22 S. Adimurthy, C. C. Malakar and U. Beifuss, *J. Org. Chem.*, 2009, **74**(15), 5648–5651.
23 F. Mohajer, M. M. Heravi and V. Zadsirjan, *RSC Adv.*, 2021, **11**, 6885–6925.
24 M. Gazvoda, M. Virant, B. Pinter and J. Košmrlj, *Nat. Commun.*, 2018, **9**, 4814, DOI: **10.1038/s41467-018-07081-5**.
25 M. Nasrollahzadeh, M. Atarod, M. Alizadeh, A. Hatamifard and S. M. Sajadi, *Curr. Org. Chem.*, 2017, **21**, 708–749.
26 V. Verdoliva, M. Saviano and S. De Luca, *Catalysts*, 2019, **9**, 248, DOI: **10.3390/catal9030248**.
27 P. Sánchez-López, Y. Kotolevich, R. I. Yocupicio-Gaxiola, J. Antúnez-García, R. K. Chowdari, V. Petranovskii and S. Fuentes-Moyado, *Front. Chem.*, 2021, 716745, DOI: **10.3389/fchem.2021.716745**.
28 M. Rose, *ChemCatChem*, 2014, **6**, 1166–1182, DOI: **10.1002/cctc.201301071**.
29 M. Xu, J. Zhao, G. Shu, Q. Liu and M. Zeng, *Polymers*, 2018, **10**, 669, DOI: **10.3390/polym1006066**.
30 A. Modak, J. Mondal, M. Sasidharan and A. Bhaumik, *Green Chem.*, 2011, **13**, 1317–1331, DOI: **10.1039/C1GC15045F**.
31 J. Liang, Z. Liang, R. Zou and Y. Zhao, *Adv. Mater.*, 2017, **29**, 1701139, DOI: **10.1002/adma.201701139**.
32 B. K. Singh, Y. Kim, S. Kwon and K. Na, *Catalysts*, 2021, **11**, 1541, DOI: **10.3390/catal11121541**.
33 L. Yin and J. Liebscher, *Chem. Rev.*, 2007, **107**, 133–173.
34 S. Vásquez-Céspedes, R. C. Betori, M. A. Cismesia, J. K. Kirsch and Q. Yang, *Org. Process Res. Dev.*, 2021, **25**(4), 740–753.
35 P. P. Mpungose, Z. P. Vundla, G. E. M. Maguire and H. B. Friedrich, *Molecules*, 2018, **23**, 1676.
36 A. H. Labulo, B. S. Martincigh, B. Omondi and V. O. Nyamori, *J. Mater. Sci.*, 2017, **52**, 9225–9248.
37 Z. Han and A. Fina, *Prog. Polym. Sci.*, 2011, **36**, 914.
38 K. Sun, M. A. Stroscio and M. Dutta, *J. Appl. Phys.*, 2009, **105**, 1.
39 J. Che, T. Cagin and W. A. Goddard III, *Nanotech*, 2000, **11**, 65.
40 P. Serp, M. Corrias and P. Kalck, *Appl. Catal., A*, 2003, **253**, 337.
41 P. Serp and E. Castillejos, *ChemCatChem*, 2010, **2**, 41.
42 Y. Yan, J. Miao, Z. Yang, F.-X. Xiao, H. B. Yang, B. Liu and Y. Yang, *Chem. Soc. Rev.*, 2015, **44**, 3295–3346.

43 B. Cornelio, G. A. Rance, M. Laronze-Cochard, A. Fontana, J. Sapi and A. N. Khlobystov, *J. Mater. Chem. A*, 2013, **1**, 8737–8744, DOI: 10.1039/C3TA11530E.
44 B. P. Chandra, Z. Wu, S. Addo Ntim, G. Nageswara Rao and S. Mitra, *Appl. Sci.*, 2018, **8**, 1511, DOI: 10.3390/app8091511.
45 A. R. Siamaki, Y. Lin, K. Woodbery, J. W. Connell and B. F. Gupton, *J. Mater. Chem.*, 2013, **1**, 12909.
46 S. K. Folsom, D. J. Ivey, F. S. McNair and A. R. Siamaki, *Catalysts*, 2021, **11**, 495, DOI: 10.3390/catal11040495.
47 Y. Lin, D. W. Bagget, J.-W. Kim, E. J. Siochi and J. W. Connell, *ACS Appl. Mater. Interfaces*, 2011, **3**, 1652–1664.
48 S. Landge, D. Ghosh and K. Aiken, *Green Chem.*, 2018, 609–646.
49 Y.-S. Feng, X.-Y. Lin, J. Hao and H.-J. Xu, *Tetrahedron*, 2014, **70**, 5249–5253.
50 X. Chen, D. Qian, G. Xu, H. Xu, J. Dai and Y. Du, *Colloids Surf., A*, 2019, **573**, 67–72.
51 Y.-H. Li, J.-Y. Li and Y.-J. Xu, *EnergyChem*, 2021, **3**, 100047.
52 M.-Y. Qi, M. Conte, M. Anpo, Z.-R. Tang and Y.-J. Xu, *Chem. Rev.*, 2021, **121**, 13051.
53 L. Chen, X. Chen, H. Liu and Y. Li, *Small*, 2015, **11**, 2642.
54 L. Chen, B. Huang, X. Qiu, X. Wang, R. Luque and Y. Li, *Chem. Sci.*, 2016, **7**, 228.
55 L. Chen, H.-F. Wang, C. Li and Q. Xu, *Chem. Sci.*, 2020, **11**, 5369.
56 R. Narayanan, *Molecules*, 2010, **15**, 2124–2138, DOI: 10.3390/molecules15042124.
57 S. E. Smith, A. R. Siamaki, B. F. Gupton and E. E. Carpenter, *RSC Adv.*, 2016, **6**, 91541–91545.
58 R. K. Rai, D. Tyagi, K. Gupta and S. K. Singh, *Catal. Sci. Technol.*, 2016, **6**, 3341–3361.
59 S. Z. Tasker, E. A. Standley and T. F. Jamison, *Nature*, 2014, **509**, 299–309.
60 V. P. Ananikov, *ACS Catal.*, 2015, **5**, 1964–1971.
61 J. Ranjan, P. P. Tejas and M. S. Sigman, *Chem. Rev.*, 2011, **111**, 1417–1492, DOI: 10.1021/cr100327p.
62 J. Chopra, A. K. Goswami and P. K. Baroliya, *Mini-Rev. Org. Chem.*, 2020, **17**(16), 589–604, DOI: 10.2174/1570193X16666190617160339.
63 J. B. Diccianni and T. Diao, *Trends Chem.*, 2019, **1**, 830–844.
64 F.-S. Han, *Chem. Soc. Rev.*, 2013, **42**, 5270–5298, DOI: 10.1039/c3cs35521g.
65 J. M. Richardson and C. W. Jones, *J. Mol. Catal. A: Chem.*, 2009, **297**, 125–134, DOI: 10.1016/j.molcata.2008.09.021.
66 M. R. Netherton and G. C. Fu, *Adv. Synth. Catal.*, 2004, **346**, 1525–1532.
67 Z. Li and L. Liu, *Chin. J. Catal.*, 2015, **36**, 3–14.
68 J. M. Weber, A. R. Longstreet and T. F. Jamison, *Organometallics*, 2018, **37**, 2716–2722.
69 N. J. S. Costa, M. Guerrero, V. Collière, É. Teixeira-Neto, R. Landers, K. Philippot and L. M. Rossi, *ACS Catal.*, 2014, **4**, 1735–1742.
70 N. Hazari, P. Melvin and M. Beromi, *Nat. Rev. Chem.*, 2017, **1**, 0025, DOI: 10.1038/s41570-017-0025.
71 S. Uk Son, Y. Jang, J. Park, H. Bin Na, H. M. Park, H. J. Yun, J. Lee and T. Hyeon, *J. Am. Chem. Soc.*, 2004, **126**(16), 5026–5027.
72 X. Cui, W. Li, P. Ryabchuk, K. Junge and M. Beller, *Nat. Catal.*, 2018, **1**, 385–397.
73 D. Han, Z. Zhang, Z. Bao, H. Xing and Q. Ren, *Front. Chem. Sci. Eng.*, 2018, **12**, 24–31.
74 R. K. Rai, K. Gupta, D. Tyagi, A. Mahata, S. Behrens, X. Yang, Q. Xu, B. Pathak and S. K. Singh, *Catal. Sci. Technol.*, 2016, **6**, 5567–5579.
75 Y. Jiang, Q. Li, X. Li, X. Wang, S. Dong, J. Li, L. Hou, T. Jiao, Y. Wang and F. Gao, *ACS Omega*, 2021, **6**, 9780–9790.
76 Y. Zhang, Y. Liao, G. Shi, W. Wang and B. Su, *Green Process. Synth.*, 2020, **9**, 760–769.
77 Y. Liao, Y. Wang and Y. Zhang, *Catalysts*, 2022, **12**, 370, DOI: 10.3390/catal12040370.